

# Design considerations for an acoustic MEMS filter

S.-H. Shen, W. Fang, S.-T. Young

585

**Abstract** Microelectromechanical system (MEMS) devices exhibit characteristics that make them ideal for use as filters in acoustic signal processing applications. In this study, a MEMS filter is constructed from multiple mechanical structures (e.g. cantilever beams) and a differential amplifier. The outputs of the structures are then processed by the differential amplifier to achieve the filter functionality. The important parameters of the mechanical structures and the MEMS filters are investigated using a simulation approach, including the structural damping factors, the normalized frequency ratios (NFR) of the MEMS filters, the number of mechanical structures required to construct individual MEMS filter, and the spatial arrangement of the multiple mechanical structures relative to the differential amplifier. Furthermore, the mutual coupling effects among these parameters are evaluated by detailed simulations. The simulation results show that a plot of the NFR versus the damping factors can be used to determine the optimal parameters for the mechanical structures. The number of mechanical structures required to construct a MEMS filter must equal  $2^n$ , with  $n$  as an integer, and these mechanical structures should be arranged as a geometric series with increasing resonant frequencies and with specific connections to the differential amplifier.

## 1 Introduction

A crucial aspect for many signal-processing techniques, including acoustic signal processing, is to divide the signal into multiple frequency bands. With its powerful computing

capabilities, the digital signal processor (DSP) now forms the core for such techniques [1, 2]. However, contemporary DSPs still present limitations for some applications, in terms of their power consumption and computation time. Where these factors are crucial, the electromechanical filter – as a passive device – provides a viable alternative. Electromechanical filters have been well known for at least 5 decades [3]. They can be used to extract signals from a specific frequency band, and hence provide functionality similar to electrical filters. Electromechanical filters also provide excellent aging and thermal-stability characteristics [4]. With the introduction of microelectromechanical systems (MEMSs), the application of electromechanical filters to signal processing has become more feasible, from high-frequency to radio-frequency regions [5–8]. An electromechanical filter bank constructed from silicon beams for a high-frequency communication system was recently investigated [9]. Each filter in this filter bank comprised a single beam structure with a sharp frequency response. A sharp frequency response always results in poor linearity for the filter passband signals.

This study proposes a novel MEMS filter for acoustic signal processing. Its characteristics and design parameters were investigated by simulations of filters comprising multiple mechanical structures. The simulation approach enabled complete characterization of the critical parameters of the mechanical structures and the MEMS filters, such as the structural damping factors, the normalized frequency ratios (NFRs) of the MEMS filters, the number of mechanical structures required to construct an individual MEMS filter, and their spatial arrangement. The simulations demonstrate that the proposed MEMS filter can be implemented, and that it would be an effective device for acoustic signal-processing applications, such as in miniature hearing aids.

## 2 Theory and methods

### 2.1 Theory on MEMS filters

A mechanical structure has a preferred vibrating mode referred to as resonance that depends on the configuration of the structure and its mechanical properties. This vibrating mode can be characterized by the magnification factor, which is taken as a normalized vibration amplitude in this paper, and phase versus frequency in the first mode of vibration, expressed as Eqs. (1) and (2), respectively [10]:

Received: 20 November 2002 / Accepted: 19 September 2003

S.-H. Shen, S.-T. Young (✉)  
Bioelectronics Laboratory, Institute of Biomedical Engineering,  
National Yang Ming University 155, Sec. 2, Li-Nung St,  
Shih-Pai, Taipei 112, Taiwan  
e-mail: Young@bme.ym.edu.tw

W. Fang  
Micro Device Laboratory, Department of Power Mechanical  
Engineering, National Tsing Hua University, Hsinchu 300,  
Taiwan

This material is based (in part) upon work supported by the National Science Council (Taiwan) under Grant NSC 91-2213-E-010-008 and Delta Electronics Foundation. The authors would like to express their appreciation to the NSC Central Regional MEMS Center, Semiconductor Research Center of National Chiao Tung University (Taiwan), and the NSC National Nano Device Laboratories (Taiwan) in providing experimental facilities.

$$\frac{|X|}{\Delta_s} = \frac{|X|}{F_0/k} = \frac{1}{\sqrt{[1 - (\omega/\omega_n)^2]^2 + [2\zeta(\omega/\omega_n)^2]^2}} \equiv \text{Magnification factor} \quad (1)$$

$$\phi = \tan^{-1} \left[ \frac{2\zeta \frac{\omega}{\omega_n}}{1 - \left(\frac{\omega}{\omega_n}\right)^2} \right] \equiv \text{Phase shift} \quad (2)$$

where  $|X|$  is the amplitude of the steady-state vibration,  $\Delta_s$  is the static displacement when the exciting force  $F_0$  is slowly applied to the mechanical structure,  $k$  is the spring constant of the structure,  $\omega_n$  and  $\omega$  are the resonance and operating frequency of the structure, and  $\zeta$  is the damping factor. In this study, micromachined cantilevers were employed to detect the acoustic waves. Hence, the  $F_0/k$  of these cantilevers with  $l$  in length and  $t$  in thickness can be expressed as Eq. (3) [11].

$$\frac{F_0}{k} = \frac{3pl^4}{2Et^3} \quad (3)$$

where  $p$  is the acoustic pressure, and  $E$  is the Young's modulus of cantilever. By dividing  $|X|$  into  $F_0/k$  using pre-signal-processing tools, such as amplifiers or programs, we can easily acquire the normalized signals.

The proposed MEMS filter is shown in Fig. 1, which consists of multiple mechanical structures with sensing

circuits and a differential amplifier. The MEMS filter had designed with a bandpass characteristic. The mechanical structures respond to acoustic stimulation, according to their particular frequency responses, and cause the sensing circuits to produce the associated electrical signals. The differential amplifier processes the electrical signals picked up from some parts of the mechanical structures. The resulting signal can be a filtered signal when the mechanical structures are designed with appropriate frequency responses and their outputs are coupled in the differential amplifier in an appropriate arrangement. For a MEMS filter with multiple mechanical structures, the output of each mechanical structures is connected to either a positive or a negative port of the differential amplifier through a switching mechanism, which is called as a positive and negative switch (PNS), as shown in Fig. 1a. It is obvious that the variety of possible PNS arrangements will increase with the number of mechanical structures in a MEMS filter. Besides, the MEMS filter can be implemented by, for example, micromachined cantilevers and piezoresistive sensing circuitry as shown in Fig. 1b.

For unobvious effects from higher-order resonance modes and convenient illustration, we only considered the first resonance mode of the mechanical structure. Combining Eqs. (1) and (2), the vibration of a mechanical structure can be presented by means of a cosine wave equation,  $x_i$ :

$$x_i = \frac{|X_i|}{\Delta_{s_i}} \cos(2\pi\omega t + \phi_i) = \frac{1}{\sqrt{[1 - (\omega/\omega_{ni})^2]^2 + [2\zeta(\omega/\omega_{ni})^2]^2}} \cos \left( 2\pi\omega t + \tan^{-1} \left[ \frac{2\zeta \frac{\omega}{\omega_{ni}}}{1 - \left(\frac{\omega}{\omega_{ni}}\right)^2} \right] \right) \quad (4)$$

The suffix  $i$  represents the label of an individual structure. Multiple mechanical structures can be designed such that their resonant frequencies increase sequentially, with their responses  $x_1, x_2, \dots, x_i$  coupled together to implement a MEMS filter. The general response of such a MEMS filter can be presented as

$$x_{total} = |x_i + \dots + x_{i-M} \dots - x_{i-N} - \dots - x_1|, \quad i \geq 2, \quad i-1 > M \geq 0, \quad i-1 > N > 0, \quad M \neq N \quad (5)$$

## 2.2

### Performance definition and evaluation of MEMS filter

We evaluated the performance of the MEMS filter by measuring certain filter parameters, including the passband ripples and the filter shape. We wanted the passband ripple to be less than 1 dB, and in any case ensure that it did not exceed 3 dB to avoid violation of the cutoff-frequency definition. The asymmetric filter shape is assessed by a defined shape factor. The shape factor of the MEMS filter was divided into the lower shape factor (LSF) and higher shape factor (HSF), which describe either side of the bandpass filter's shape. LSF and HSF are defined in

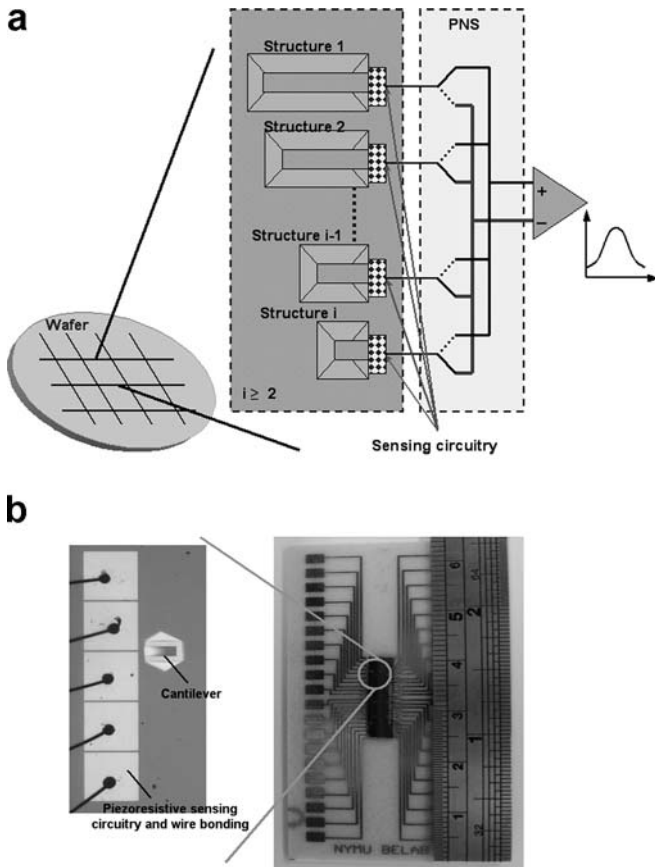


Fig. 1a, b. Illustrations of MEMS filters: a a concept diagram of the proposed MEMS filter; b a practical MEMS filter with micromachined cantilevers and piezoresistive sensing circuitry

Eqs. (6) and (7), respectively, and the related definitions are illustrated in Fig. 2. According to our definitions, a MEMS filter with lower LSF and HSF values has a sharper passband, and the filter is more symmetric when its LSF and HSF values are similar:

$$\text{LSF} = \frac{\text{The logarithmic bandwidth between } f_0 \text{ and } f_{L,-40\text{dB}}}{\text{The logarithmic bandwidth between } f_0 \text{ and } f_L} = \frac{\log(f_0) - \log(f_{L,-40\text{dB}})}{\log(f_0) - \log(f_L)} \quad (6)$$

$$\text{HSF} = \frac{\text{The logarithmic bandwidth between } f_0 \text{ and } f_{H,-40\text{dB}}}{\text{The logarithmic bandwidth between } f_0 \text{ and } f_H} = \frac{\log(f_{H,-40\text{dB}}) - \log(f_0)}{\log(f_H) - \log(f_0)} \quad (7)$$

where  $f_L$  is the lowest resonant frequency and  $f_H$  is the highest resonant frequency of the structures comprising the MEMS filter; and  $f_0$  is the center frequency, equal to the average of  $f_L$  and  $f_H$ ;  $f_{L,-40\text{dB}}$  and  $f_{H,-40\text{dB}}$  are the upper and lower frequencies at which 40-dB attenuations occur.

### 2.3 Simulation approach

Using Eqs. (4) and (5), we developed simulation programs to explore the optimized design parameters of the proposed MEMS filter, using the following criteria:

- The damping factors of the mechanical structures are the first parameters to be investigated, since their combination will determine the passband ripple and resonant frequency of the MEMS filter. We simulated different individual damping factors and different combined ratios.
- The bandwidth is the second important parameter for the MEMS filter. The bandwidth investigation is achieved through the NFR. The NFR of a MEMS filter constructed by multiple mechanical structures with increasing resonant frequencies  $f_1, f_2, \dots, f_n$  is described by the normalized interval between the lowest resonant frequency  $f_L (= f_1)$  and the highest resonant frequency  $f_H (= f_n)$  of the MEMS filter. The NFR is defined as

$$\text{NFR} = \frac{\text{Center frequency}}{\text{The bandwidth between } f_H \text{ and } f_L} = \frac{\frac{1}{2}(f_H + f_L)}{f_H - f_L} = \frac{f_0}{f_H - f_L} \quad (8)$$

The center frequency  $f_0$  is the average of  $f_L$  and  $f_H$ . By the definition, the NFR is inversely proportional to the bandwidth for the same center frequency. How the NFR effects the MEMS filter was also fully investigated by the simulation program.

- Once the desired damping factors and filter bandwidth were determined, the mechanical structures comprising the MEMS filter were determined by simulations. Different relationships between these structures and the differential amplifier were also analyzed. These were implemented by configuring the PNS shown in Fig. 1. For clarity of illustration, when the PNS links the mechanical structure to the positive port of the differential amplifier, the structure is symbolized as a positive sign (“+”); whereas when the PNS switches to the negative port, the structure is symbolized as a negative sign (“-”). The sequential presentation of these signs in the MEMS filter indicates the mechanical structures with increasing resonant frequencies.
- The effects of the individual parameters on the characteristics of the MEMS filter are not independent, and hence their mutual effects on each other were also investigated in the study. The simulations analyzed the relationships between the damping factors and the NFR to explore their trade-off whilst maintaining an acceptable passband ripple. The simulations also thoroughly investigated the effects on the filter shape factors of NFR and number of structures simultaneously to determine a reasonable number of mechanical structures for the MEMS filter.

## 3 Simulation results

The results of simulations into the effects of the damping factor, the NFR, and the number of mechanical structures comprising the MEMS filters are presented in Sects. 3.1–3.4, respectively. For illustrative simplicity, 2-structure MEMS filters are used to show the effects of damping factors and NFR in Sects. 3.1 and 3.2. The simulation results for multiple-structure MEMS filters are only depicted with an NFR of 2.50 and a damping factor of 0.123; for these values the 2-structure MEMS filter exhibits a passband ripple of only 1 dB in Sect. 3.3. The resonant frequencies of adjacent structures are arranged as a geometric series in multiple-structure filters. The mutual relationships among the parameters and performance of MEMS filters are then illustrated in Sect. 3.4.

### 3.1 Effects of damping factor

Figure 3 illustrates how the damping factors of the structures affect the frequency response of the MEMS filter with center frequency,  $f_0$ , 1000 Hz. In Fig. 3a, the damping factors of two structures,  $\zeta_L$  and  $\zeta_H$ , were assigned values of 0.123 and 0.984 ( $\zeta_H = 8\zeta_L$ ), 0.984 and 0.123 ( $\zeta_L = 8\zeta_H$ ),

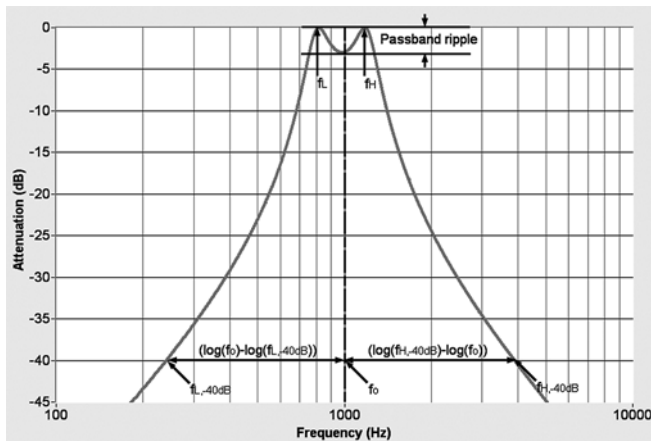


Fig. 2. Illustration of the definitions of MEMS filter parameters

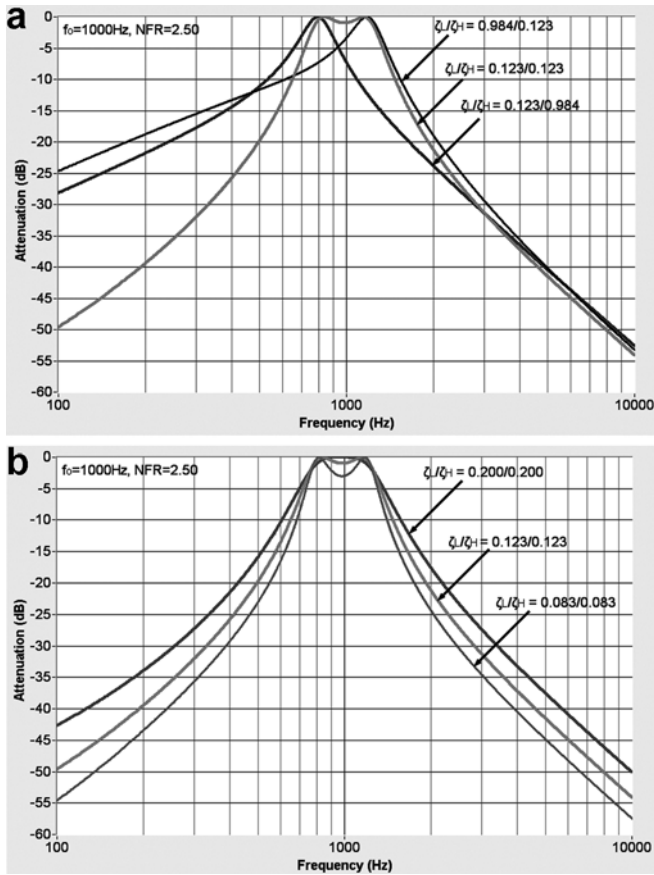


Fig. 3a, b. The effect of damping factors on the frequency responses of MEMS filters comprised of two structures with: a different damping factors and, b the same damping factor

and 0.123 and 0.123 ( $\zeta_L = \zeta_H$ ), respectively. Figure 3b shows the response of MEMS filters that were comprised of two structures with equal damping factors of 0.083, 0.123, and 0.200. The resulting LSF, HSF, and passband-ripple values for these MEMS filters were 6.37, 7.45, and 3 dB; 7.35, 8.38, and 1 dB; and 9.28, 9.56, and 0 dB; respectively.

### 3.2

#### Effects of normalized frequency ratio

Figure 4 shows the effect of different NFRs on the frequency response of MEMS filters. Figure 4a shows that NFR values of 1.69, 2.50, and 3.90 produce MEMS filters with LSF, HSF, and passband-ripple values of 7.36, 8.39, and 3 dB; 7.35, 8.38, and 1 dB; and 10.16, 11.04, and 0 dB; respectively. Figure 4b illustrates the frequency responses of different MEMS filters that have center frequencies of 500 Hz, 1000 Hz, and 3000 Hz, but the same NFR and damping factors of 2.50 and 0.123, respectively. These MEMS filters produce identical LSF, HSF, and passband-ripple values, of 7.35, 8.38, and 1 dB, respectively.

### 3.3

#### Effects of number of mechanical structures and their arrangement

Figure 5 illustrates the frequency responses of 4-structure MEMS filters, whose structures had resonant frequencies of 800 Hz, 916 Hz, 1048 Hz, and 1200 Hz (i.e.,  $f_L = 800$  Hz

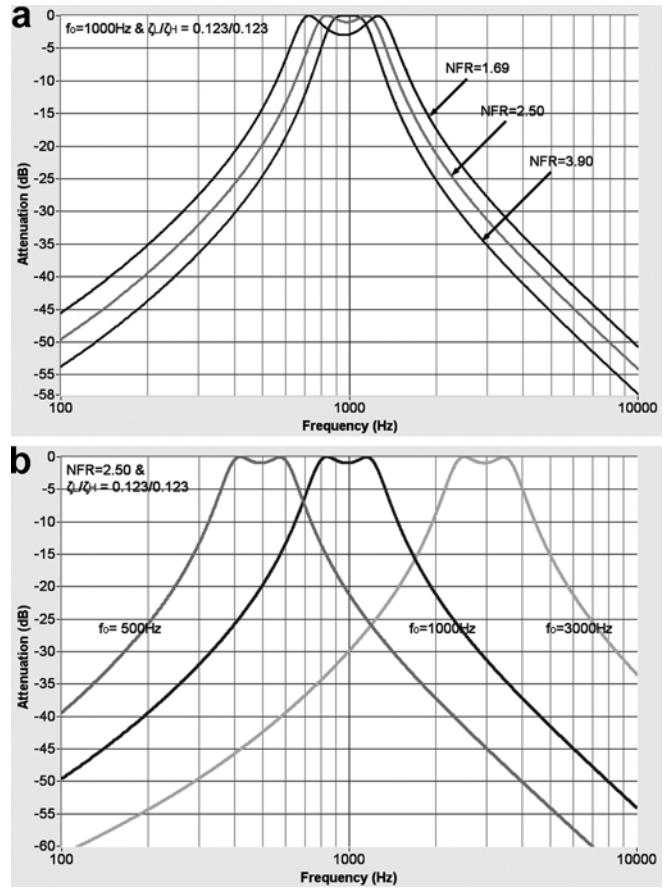


Fig. 4a, b. The effect of NFR on the frequency responses of MEMS filters: a with various NFRs but with the same center frequency and damping factor; b with different center frequency  $f_0$  but with the same NFRs and damping factors

and  $f_H = 1200$  Hz). The figure shows the responses of the 4-structure MEMS filters for only some of the possible structure arrangements, which were arranged with equal structures to connect to both ports of the differential amplifier. The LSFs, HSFs, and passband-ripple values of the 4-structure MEMS filters are 4.35, 5.10, and 0.32 dB, for the “+ - + -” PNS arrangement; 7.04, 8.05, and 22.95 dB for “+ - + -”; and 6.75, 7.73, and 0 dB for “+ + - -”.

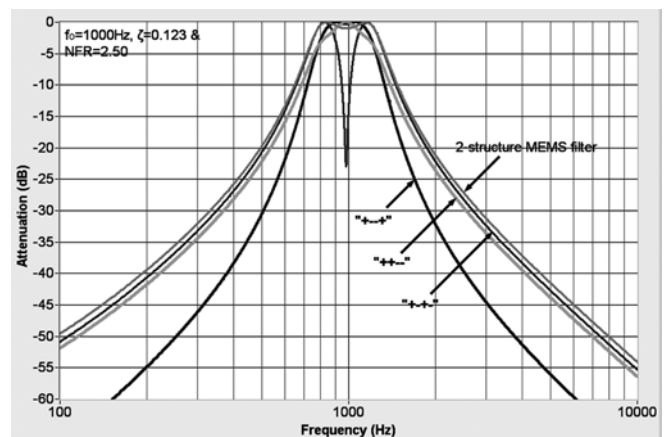


Fig. 5. The frequency responses of 4-structure MEMS filters with different structure arrangements

Figure 6 shows the best frequency responses of 6-, 8-, 12-, and 16-structure MEMS filters, for PNS arrangements of “+ - - + + -”, “+ - - + - + + -”, “+ - - + - + + - + - + - + - + - + - + -”, and “+ - - + - + + - - + + - + - + - - +”, respectively. The LSF and HSF values for 8-, 12-, and 16-structure MEMS filters were 3.02 and 3.47; 2.88 and 3.3; and 2.46 and 2.78; respectively, while the passband-ripple values were 1 dB, 0 dB, and 3.43 dB, respectively. The responses of the 8- and 12-structure MEMS filters intersect around 380 Hz and 2650 Hz. Due to the serious asymmetry to the central frequency axis of its response, the passband-ripple values and shape factors cannot be defined in the 6-structure MEMS filter.

Figure 7 depicts the responses of 8- and 16-structure MEMS filters with different center frequencies and the same NFR of 2.5. The center frequencies were set as 500 Hz, 1000 Hz, and 3000 Hz, and the PNS arrangements were set as “+ - - + - + + -” and “+ - - + - + + - - + + - + - + - - +”. The LSF, HSF, and passband-ripple value of the 8-structure MEMS filters are 3.02, 3.47, and 1 dB, and those of the 16-structure MEMS filters are 2.46, 2.78, and 3.43 dB.

**3.4 Mutual effects among crucial parameters**

For passband-ripple values of 1 dB and 3 dB, Fig. 8 shows that the damping factors and the NFRs were inversely relationships irrespective of the number of the mechanical structures used to construct the MEMS filter. The mutual relationship of NFRs in 4-, 8-, and 16-structure MEMS filters, and damping factors and filter shape factors are illustrated in Fig. 9 for 1-dB and 3-dB passband ripples. These figures show the trade-off between the shape factors LSF and HSF with different desired NFRs.

**4 Discussion**

As designing a MEMS filter constructed from mechanical structures, it is necessary to define its center frequency, filter bandwidth, acceptable passband ripple, and desired filter shape. The characteristics of a MEMS filter are

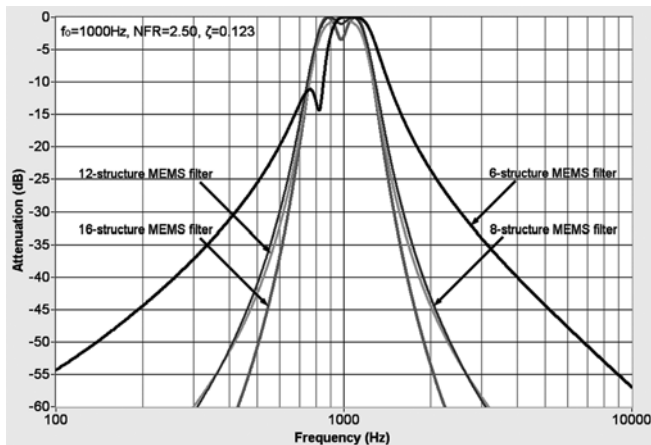


Fig. 6. The best frequency responses in 6-, 8-, 12-, and 16-structure MEMS filters

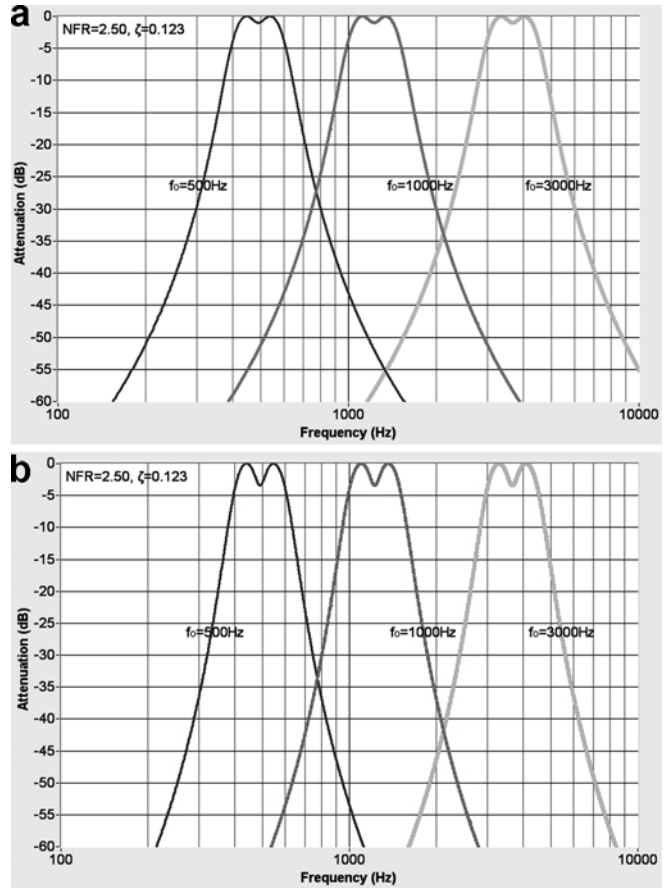


Fig. 7a, b. The frequency responses of MEMS filters constructed by multiple structures with the same damping factor and NFR, but various center frequencies: a 8-structure MEMS filters; b 16-structure MEMS filters

affected by many parameters, including the damping factors of the mechanical structures, the NFRs, and the number and arrangement of mechanical structures constituting the filter. This study investigated these parameters by simulating various MEMS filters, and the results provide certain guidelines for the design of such filter.

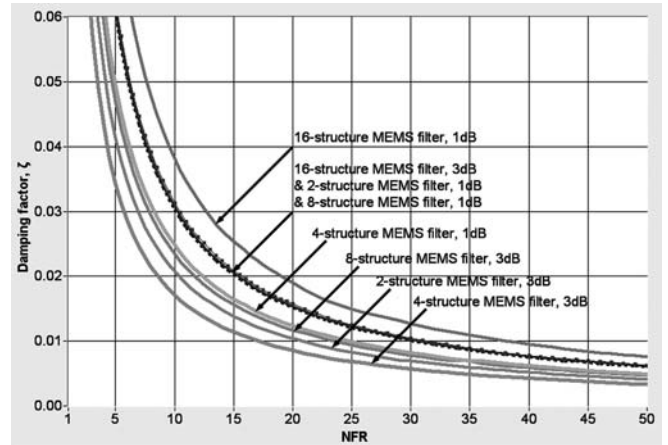


Fig. 8. The relationship between NFRs and damping factors with differing numbers of structures and passband-ripple values

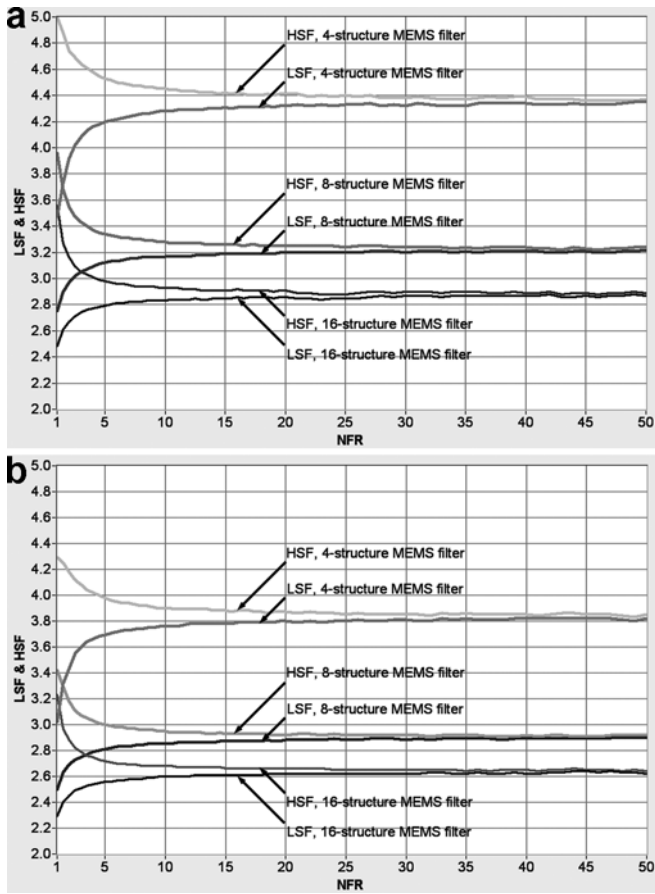


Fig. 9a, b. The relationship between NFR and shape factors for a response: **a** with a 1-dB passband ripple and different numbers of structures and, **b** with a 3-dB passband ripple and different numbers of structures

The damping factor of the mechanical structure is one of these important parameters. The simulation results showed that the damping factors of the mechanical structures should be as similar as possible to ensure the symmetry of the frequency response of the MEMS filter. When a MEMS filter is made from structures with unbalanced damping factors, its filter profile will skew to the frequency response of the structure with the lower damping factor. The more unbalanced the damping factors are, the more asymmetric the filter profile appears; and in extreme cases the filter may lose its filtering functionality, with undefined LSF and HSF values. Moreover, appropriate damping factors are evidently necessary: a larger damping factor decreases the passband ripples but enlarges the LSF and HSF, when NFR is kept constant; whereas a small damping factor produces a MEMS filter with small LSF and HSF. However, damping factors that are too small will produce a MEMS filter with individual mechanical structures that do not exhibit mutual coupling.

The NFR of the MEMS filter is another important parameter – it essentially determines the bandwidth of the MEMS filter. Increasing the NFR both narrows the filter bandwidth and makes the passband ripple smaller. The simulation results also revealed the interesting characteristic that MEMS filters with identical NFRs and damping factors will have identical passband ripples and shape

factors, even though they can have different center frequencies. This will simplify the design of MEMS filters for use at different frequencies. Furthermore, the NFR and the damping factor have mutual effects on the MEMS filter. The simulation results (in Fig. 8) show that the damping factor and the NFR are inversely related, which is important information when designing for the allowable passband ripple and desired shape factor of the MEMS filter: to decrease the bandwidth of a MEMS filter it is necessary to decrease the damping factor whilst simultaneously increasing the NFR.

The number and arrangement of the structures is especially important in the construction of multiple-structure MEMS filters. The simulations showed that the mechanical structures in a MEMS filter must be arranged in a mirror relationship to the differential amplifier (e.g. “+ – + – + –” for eight structures and “+ – + – + + – – + + – – +” for 16 structures. This arrangement can be explained with reference to logic. A 2-structure MEMS filter has its basic arrangement as “+ –” (or “– +”). For a 4-structure MEMS filter, its best PNS arrangement is “+ – + –”, which can be considered as two adjacent subsets, “+ –” and “– +”. Each subset can be taken as a new structure, with the subset “– +” being regarded as the inverse of “+ –”. The combination of the two subsets can then be considered as another 2-structure MEMS filter arranged with the mirror relation “+ –”. Following this arranging rule, the best arrangement of an 8-structure MEMS filter is then derived from the combination of subset “+ – – +” and its inverse “– + + –”, and the best arrangements of the 16-structure MEMS filter is predicted as the combination of “+ – – + – + + –” and “– + + – + – – +”. The mirror relation in this best PNS arrangement implies that the number of structures in a MEMS filter must be equal to  $2^n$ , where  $n$  is an integer. This also means that the train of the arrangement can be folded up until it has its basic arrangement as “+ –”. Although the multiple-structure MEMS filter can be regarded as a pair of structures that process the incoming signals, each virtual structure exhibits damping that is different from that exhibited by the preceding structure combination; therefore, this study has not provided a complete comparison between 2-structure and multiple-structure MEMS filters.

The mutual effects of all parameters on the MEMS filters were very important when designing the filter proposed in the study. The damping factor of each structure within the filter is determined by both structural and environmental factors, with changes in environmental conditions being more significant at micron dimensions. The squeezed-film effect is often taken as the critical solution for tuning the damping factors in microstructures. Based on the squeezed-film theory, the gap depth and covered area of the microstructure – as controlled by the fabrication process – enables any damping factors to be obtained; for instance, the stationary structures proposed in [12] can be employed to tune the quality factor of bulk micro-machined structures by incorporating with the squeezed-film damping. However, using a single damping factor for all the structures is expected to simplify the fabrication of the proposed MEMS filter on a wafer. In this case, the

number of structures becomes as a major selectable parameter for obtaining the desired passband ripple and bandwidth. Figure 8 shows that with a fixed damping factor, increasing the number of structures will increase NFR and decrease passband ripple, except in the 2-structure MEMS filter. Increasing NFR decreases the bandwidth. A large number of structures will also decrease LSF and HSF values, as shown in Fig. 9, and the decreasing LSFs and HSFs produces a sharper filter. A large number of structures will then enhance the filter performance. Another interesting phenomenon is that increasing NFR will increase the LSF but decrease the HSF. This trend brings the LSF and HSF closer, producing a more symmetrical filter. However, the advantages of increasing the number of mechanical structures do not continue indefinitely: too many mechanical structures will complicate the filter fabrication and decrease the yield rate. We therefore propose that an 8-structure MEMS filter represents the best compromise.

## 5 Summary and conclusions

This paper has proposed the design of a MEMS filter and investigated its important parameters using a simulation approach. In theory, all the requirements of MEMS filters can be satisfied through the selection of appropriate damping factors of the mechanical structures, NFR, and the number and arrangement of the mechanical structures that constitute the filter. For individual MEMS filter with multiple mechanical structures, the structures should have similar damping factors. The NFR of the MEMS filter is another important parameter, which determines the filter shape and bandwidth for different center frequencies. Furthermore, the simulation results show that the number of mechanical structures required to construct a MEMS filter must be a power of 2, and the resonant frequencies of these structures should be arranged as a geometric series. These mechanical structures are connected to a differential amplifier, and their PNS arranged using a mirror relationship. The fine tuning of these parameters allows the desired filter characteristics to be realized step by step. The

filter designer can follow the design rules in this paper to easily construct a MEMS filter with the desired functionality. The MEMS filter provides not only the advantages of MEMS technology but also a creative and feasible concept for acoustic signal processing which represents a viable alternative to DSP implementations, with advantages of lower power consumption and shorter computation time. We firmly believe that these novel MEMS filters represent promising new devices for acoustic signal processing.

## References

1. McDermott H (1998) A programmable sound processor for advanced hearing aid research. *IEEE Transac Rehabil Eng* 6(1): 53–59
2. Mitchell J; Pruehsner W; Enderle JD (1999) Digital hearing aid. *Proceedings of the IEEE 25th Annual Northeast Bioengineering Conference*. pp. 133–134, connecticut
3. Adler R (1947) Compact electromechanical filter. *Electronics*. 20: 100–105
4. Johnson RA (1983) *Mechanical filters in electronic*. John Wiley & Sons, New York
5. Lin L; Howe RT; Pisano AP (1998) Microelectromechanical filters for signal processing. *J Microelectromech Sys* 7(3): 286–294
6. Nguyen CTC (1999) Frequency-selective MEMS for miniaturized low-power communication devices. *IEEE Trans Micro The Tech* 47(8): 1486–1503
7. Yang LJ; Huang TW; Chang PZ (2001) CMOS microelectromechanical bandpass filters. *Sens Actua A90*: 148–152
8. Wang K; Nguyen CTC (1997) High-order micromechanical electronic filters. *Proceedings of the IEEE Tenth Annual International Workshop on Micro Electro Mechanical Systems*. pp. 25–30, Nagoya, Japan
9. Hribšek MF (1996) Electromechanical silicon beam filter bank. *Microelec J* 27: 525–530
10. James ML; Smith GM; Wolford JC; Whaley PW (1994) *Vibration of mechanical and structural systems*. 2nd edn. HarperCollins, New York
11. Beer FP; Johnson ER (1992) *Mechanics of materials*. 2nd edn. McGraw-Hill, New York
12. Cheng CC; Fang W (2003) Tuning the Quality Factor of Micromachined Bulk-Silicon Micromachined Structures Using the Squeezed- Film Damping. *12th International Conference on Solid-States, Sensors, Actuators and Microsystems (Transducers' 03)*. pp. 1590–1593, Boston, USA